Particle Accelerators, 1990, Vol. 29, pp. 159–165
Reprints available directly from the publisher
Photocopying permitted by license only

ANALYSIS OF COAXIAL WIRE MEASUREMENT OF LONGITUDINAL COUPLING IMPEDANCE[1]

R.L. GLUCKSTERN AND R. LI
Physics Department, University of Maryland, College Park, MD, USA

I. INTRODUCTION

In recent work[2], a method has been developed to calculate the longitudinal impedance for an azimuthally symmetric obstacle in a beam pipe of circular cross section. The method has been applied to a small obstacle[3], to an obstacle of general shape at high frequency[2], and to several obstacles, including a periodic structure[4,5] at high frequency.

Coupling impedances are difficult to measure directly. Instead, the reflection and transmission coefficients for a pulse carried through the obstacle on a thin coaxial wire are measured and the results approximate the longitudinal coupling impedance.[6]

In the present paper, an analysis is carried out including the coaxial wire and new boundary conditions for the fields at the surface of the wire. We then estimate the validity of the coaxial wire measurement for a variety of frequencies and geometries. Finally, several numerical calculations are carried out for both the beam and the wire pulse. The results confirm the predictions of the analysis.

II. ANALYSIS FOR A BEAM

Let us consider a beam pipe of radius a which enters and leaves an azimuthally symmetric cavity of general shape. The longitudinal impedance can be obtained by field matching at r = a. The source fields in the ultrarelativistic limit are

$$E_z^{(s)} = 0 \ , \ Z_o H_\varphi^{(s)} = -\frac{Z_o I_o}{2\pi r} e^{-jkz} = -E_r^{(s)} \ . \tag{2.1}$$

Adding the pipe fields, we find

$$E_z = \int_{-\infty}^{\infty} dq \ A(q) \ e^{-jqz} \frac{J_o(Kr)}{J_o(Ka)} \ , \tag{2.2}$$

$$Z_oH_\phi = -\frac{Z_oI_o}{2\pi r}\, e^{-jkz} - jk\int_{-\infty}^{\infty} dq\ A(q)\ e^{-jqz}\,\frac{J_o'(Kr)}{KJ_o(Ka)}\ . \tag{2.3}$$

Here $k = \omega/c$, the suppressed time dependence is $\exp(j\omega t)$, $Z_o = 120\pi$ ohms, and I_o is the driving current. We have defined $K = \sqrt{k^2 - q^2}$ and take the contour in the q plane below the poles on the negative real axis and above the poles on the positive real axis so that we have only outgoing waves for the pipe fields as $z \to \pm\infty$. Defining $E_z(a,z) \equiv f(z)$, we have

$$f(z) = \int_{-\infty}^{\infty} dq\ A(q)\ e^{-jqz}\ ,\quad A(q) = \frac{1}{2\pi}\int_o^g dz\ f(z)\ e^{jqz}\ , \tag{2.4}$$

where $f(z)$ vanishes for $z < 0$, $z > g$.

The fields in the annular cavity region for $r \geq a$ are expanded into an orthonormal set of cavity modes[3] which satisfy metallic boundary conditions on the outer wall of the cavity as well as at $r = a$. Matching the magnetic field in the pipe and cavity regions leads to

$$\int_o^g dz'\ F(z')\left[K_p(z' - z) + K_c(z,z')\right] = j\ e^{-jkz}\ , \tag{2.5}$$

where the pipe and cavity kernels are

$$K_p(u) = \int_{-\infty}^{\infty} dq\ e^{-jqu}\ \hat{J}(q)\ ,\quad K_c(z,z') = 4\pi^2\sum_\ell \frac{h_\ell(z)\ h_\ell(z')}{k^2 - k_\ell^2}\ . \tag{2.6}$$

Here $h_\ell(z)$ is the normalized magnetic field in mode ℓ at $r = a$, $f(z) = F(z)\ Z_oI_o/ka^2$, and $\hat{J}(q)$ is defined in Eq. (2.7). The sum in Eq. (2.6) is over all azimuthally symmetric modes in the annular cavity.

We can obtain a more explicit form for $K_p(u)$ in Eq. (2.6) by using the identity

$$\hat{J}(q) \equiv \frac{J_o'(Ka)}{Ka\ J_o(Ka)} = -\,2\sum_{s=1}^{\infty}\frac{1}{q^2a^2 - b_s^2}\ . \tag{2.7}$$

where j_s are the zeroes of $J_o(x)$, and where $b_s^2 = k^2a^2 - j_s^2 = -\beta_s^2$. For positive u, the contour in Eq. (2.6) can be closed in the lower half plane, enclosing the poles at $qa = b_s$ and $qa = -j\beta_s$. For negative u, the contour encloses the poles at $qa = -b_s$ and $qa = j\beta_s$. The result for $K_p(u)$ is then

$$K_p(u) = \frac{2\pi j}{a} \sum_{s=1}^{\infty} \frac{e^{-jb_s|u|/a}}{b_s} \tag{2.8}$$

where $b_s \to -j\beta_s$ when $j_s > ka$.

The longitudinal impedance of the cavity can be written as

$$\frac{Z(k)}{Z_o} = \frac{1}{Z_o I_o} \int_{-\infty}^{\infty} dz\, e^{jkz}\, E_z(0,z) = \frac{2\pi\, A(k)}{Z_o I_o} = \frac{1}{ka^2} \int_o^g dz\, F(z)\, e^{jkz} . \tag{2.9}$$

The solution of Eq. (2.5) for F(z′) can then be used to obtain the impedance by means of Eq. (2.9).

III. ANALYSIS FOR A COAXIAL WIRE

We now start with a TEM mode in the beam pipe including a coaxial wire of radius r_o, described by

$$\tilde{E}_z = 0 \ , \ Z_o \tilde{H}_\phi = - \frac{Z_o I_o}{2\pi r} e^{-jkz} = -\tilde{E}_r \ , \tag{3.1}$$

where ~ stands for the coaxial wire case and where we have normalized to make Eq. (3.1) identical to Eq. (2.1). Adding the pipe fields, we find

$$\tilde{E}_z = \int_{-\infty}^{\infty} dq\ \tilde{A}(q) e^{-jqz} \frac{F_o(Kr)}{F_o(Ka)} , \tag{3.2}$$

$$Z_o \tilde{H}_\phi(r,z) = - \frac{Z_o I_o}{2\pi r} e^{-jkz} + jk \int_{-\infty}^{\infty} dq\ \tilde{A}(q)\ e^{-jqz} \frac{F_1(Kr)}{K\, F_o(Ka)} , \tag{3.3}$$

where the linear combinations

$$F_o(x) = Y_o(x) - \mu\, J_o(x) \ , \ F_1(x) = Y_1(x) - \mu\, J_1(x) \ , \tag{3.4}$$

with $\mu = Y_o(Kr_o)/J_o(Kr_o)$, are chosen to satisfy the boundary condition on the surface of the wire. The contour in the q plane is as before in order that we only have outgoing waves for the pipe fields.

The analysis continues as in Section II. The only difference is that $\hat{J}(q)$ in Eq. (2.7) is now

$$\tilde{J}(q) = -\frac{1}{Ka}\left(\frac{Y_1(Ka) - \mu J_1(Kr_o)}{Y_o(Ka) - \mu J_1(Kr_o)}\right) . \tag{3.5}$$

The function $\tilde{J}(q)$ is analytic in q or K, except for a second order pole at K=0 (first order poles at q=±k), and first order poles at the zeros of the denominator of Eq. (3.5). We can then write $\tilde{J}(q)$ as a sum over these poles by finding the appropriate residues, obtaining finally

$$\tilde{J}(q) = -2\sum_{s=0}^{\infty}\frac{\alpha_s}{q^2a^2 - \tilde{b}_s^2} , \tag{3.6}$$

where $\tilde{b}_s^2 = k^2a^2 - i_s^2 = -\tilde{\beta}_s^2$, and where

$$\alpha_s = \frac{J_o^2(r_o i_s/a)}{J_o^2(r_o i_s/a) - J_o^2(i_s)} , \quad s \geq 1 , \quad \alpha_o = \frac{1}{2\,\ell n(a/r_o)} . \tag{3.7}$$

Here i_s is the value of Ka at the zeroes of $F_o(Ka)$, with $i_o \equiv 0$. The pipe kernel is therefore

$$\tilde{K}_p(u) = \frac{2\pi j}{a}\sum_{s=0}^{\infty}\frac{\alpha_s}{\tilde{b}_s} e^{-j\tilde{b}_s|u|/a} . \tag{3.8}$$

The expression for the magnetic field in the cavity region is identical to that for the case of a beam on axis, since the boundary conditions are not affected by the presence of the wire. The integral equation for the axial electric field at the beam pipe is therefore

$$\int_o^g dz'\, \tilde{F}(z')\left[\tilde{K}_p(|z'-z|) + K_c(z,z')\right] = j\, e^{-jkz} , \tag{3.9}$$

with $\tilde{K}_p$ being given by Eq. (3.8) and K_c by Eq. (2.6).

In order to obtain the transmission and reflection coefficients, it is simplest to examine Eq. (3.3) for large positive and negative z. The TEM (coaxial) modes correspond to the poles at $q = \pm k$. Specifically one obtains

$$Z_o \tilde{H}_\phi^{TEM} = - \frac{Z_o I_o}{2\pi r} + \frac{2\pi\ \alpha_o A(\pm k)\ e^{\mp jkz}}{r} , \tag{3.10}$$

where the $\pm$ is for the pipe region with $z \gtrless 0$. Using Eq. (2.4), we obtain for the reflection and transmission coefficients

$$1 - T(k) = \frac{2\pi\alpha_o}{ka^2} \int_o^g dz\ \tilde{F}(z)\ e^{jkz} , \quad R(k) = \frac{2\pi\alpha_o}{ka^2} \int_o^g dz\ \tilde{F}(z)\ e^{-jkz} , \tag{3.11}$$

where we have again used $\tilde{f}(z) = \tilde{F}(z)\ Z_o I_o / ka^2$.

Comparison of Eq. (3.11) with Eq. (2.9) shows why the impedance corresponds more closely to the transmission coefficient rather than the reflection coefficient, particularly at frequencies for which $kg \geq 1$. In fact the correspondence is

$$1 - T(k) \rightarrow \frac{\pi}{\ell n(a/r_o)} \frac{Z(k)}{Z_o} . \tag{3.12}$$

IV. <u>COMPARISON OF 1-T(k) AND $2\pi\alpha_o Z(k)/Z_o$</u>

The difference between the coupling impedance and $1 - T(k)$ for the pulse on the wire is <u>totally</u> contained in the modified pipe kernel in Eq. (3.8). Specifically we have an additional term proportional to $[\ell n(a/r_o)]^{-1}$, a shift of the zeroes from j_s to i_s , and the modified coefficients α_s. For $r_o/a \ll 1$, it is easy to show that

$$i_s \cong j_s + \pi/2L_s , \quad s \geq 1 , \quad L_s = \ell n(2a/r_o j_s) - \gamma , \tag{4.1}$$

where $\gamma = .577$ is Euler's constant. Also $\alpha_s^{-1} \cong 1 - \pi/2j_s L_s^2$ for $s \geq 1$. Thus all changes are proportional to $[\ell n(a/r_o)]^{-1}$ or smaller, suggesting that there may be differences of order 20%, even for r_o/a as small as .01.

The result for a small obstacle of cross sectional area Δ may be taken directly from earlier work.[3] Specifically we can write

$$\frac{2\pi\ \alpha_o}{1 - T(k)} = 2\pi ka \left[- \frac{j}{k^2\Delta} + \sum_{s=0}^{\infty} \frac{\alpha_s e^{-j\tilde{b}_s g/a}}{\tilde{b}_s} + j\ \frac{2\ell n2}{\pi} \right] . \tag{4.2}$$

We therefore expect that the primary difference for a small obstacle will be a shift in the frequency at which the singular behavior occurs from $ka = j_s$ to i_s. This is confirmed in Figs. 1a and 1b where we plot the real and imaginary parts of $Y(k)$ and $2\pi\alpha_o[1 - T(k)]^{-1}/Z_o$ for a pill box of length $g = .05a$ and width $b-a = .1a$ for $r_o/a = .01$. The corresponding results for $r_o/a = .1$ are shown in Figs. 2a and 2b. The numerical results are obtained with programs which expand the fields in the pipe region and the cavity plus pipe region into traveling axial waves. The figures clearly show that the details of the two results differ, but that the average over the sawtooth behavior is essentially unmodified.[7]

The result at high frequency is similarly easy to predict. In earlier work, we showed[2] that the average behavior of the impedance at high frequency is obtained by converting the sum over s in the pipe kernel to an integral over s, and that the main contributions come from s of order $(ka^2/g)^{1/2}$. Since the spacing of the zeroes is essentially unmodified, we expect no significant difference in the average behavior at high frequency. This is confirmed in Figs. 3a and 3b for the real and imaginary parts of $Z(k)$ and $Z_o[1 - T(k)]/2\pi\alpha_o$ for $g/a = \pi/4$, $b/a = 1.5$, $r_o/a = .1$. What is remarkable is that the complicated oscillatory behavior is duplicated as well.

V. SUMMARY

We have derived the integral equation for the transmission coefficient of the coaxial mode for a pulse along a wire on the axis of a beam pipe and cavity. The only difference between this equation and the one for the longitudinal coupling impedance is in the pipe kernel and is of order $[\ell n(a/r_o)]^{-1}$ or less. Specific predictions are made for the comparison between $Z(k)/Z_o$ and $[1 - T(k)]/2\pi\alpha_o$ for both a small obstacle, and for a larger obstacle at high frequency, and these are confirmed by numerical calculations. Our conclusion is that measurement of $Z_o[1 - T(k)]/2\pi\alpha_o$ corresponds remarkably well to the actual longitudinal coupling impedance.

VI. ACKNOWLEDGMENT

The authors would like to express their appreciation to Filippo Neri for helpful conversations.

VII. REFERENCES

1. Work supported by the Department of Energy.
2. R.L. Gluckstern, Phys. Rev. D, 39, 2732 (1989).
3. R.L. Gluckstern and F. Neri, Longitudinal Coupling Impedance of a Small Obstacle, Proceedings of the Particle Accelerator Conference, Chicago,

IL, March 1989.
4. R.L. Gluckstern, High Frequency Behavior of the Coupling Impedance for a Large Number of Obstacles, Proceedings of the Particle Accelerator Conference, Chicago, IL, March 1989.
5. R.L. Gluckstern, Phys. Rev. D, 39, 2780 (1989).
6. See, for example, H. Hahn and F. Pederson, On Coaxial Wire Measurements of the Longitudinal Coupling Impedance, BNL Report No. 50870 (1978).
7. The erratic nature of a few of the singularities is due to the cut off in mode number and the frequency step used in the numerical calculation.

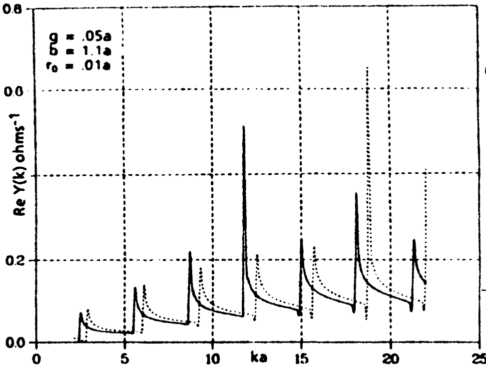

Figure 1a. Real part of admittance for a beam (solid curve) and a coaxial wire of radius r_0 = .01a (dashed curve).

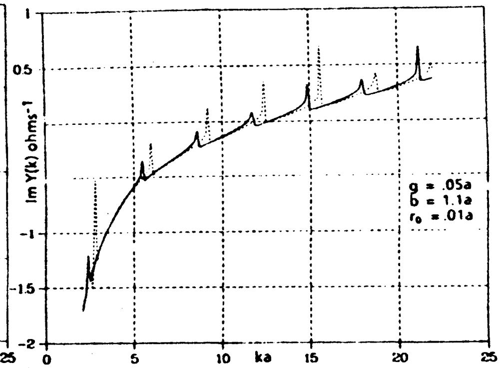

Figure 1b. Imaginary part of admittance for a beam (solid curve) and a coaxial wire of radius r_0 = .01a (dashed curve).

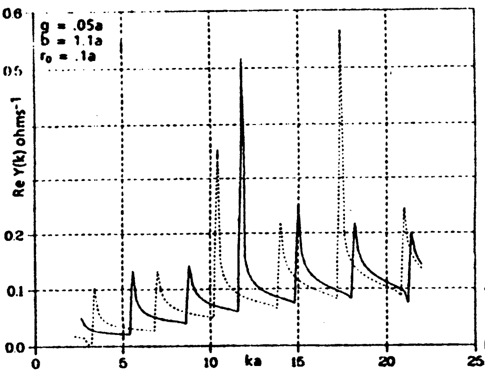

Figure 2a. Real part of admittance for a beam (solid curve) and a coaxial wire of radius r_0 = .1a (dashed curve).

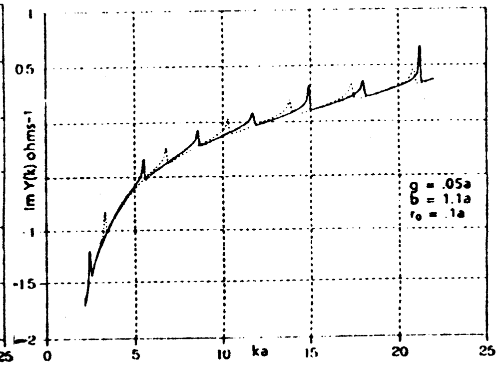

Figure 2b. Imaginary part of admittance for a beam (solid curve) and a coaxial wire of radius r_0 = .1a (dashed curve).

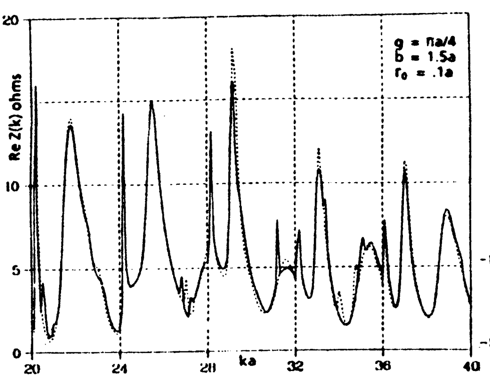

Figure 3a. Real part of impedance for a beam (solid curve) and coaxial wire of radius r_0 = 1a (dashed curve)

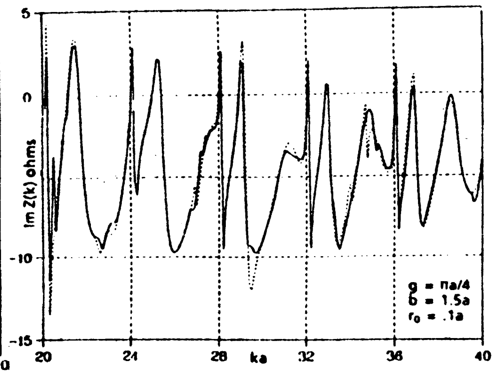

Figure 3b. Imaginary part of impedance for a beam (solid curve) and coaxial wire of radius r_0 = .1a (dashed curve).